Second-Surface Silvered Glass Solar Mirrors of Very High Reflectance

Guillaume P. Butel[a], Blake M. Coughenour[a], H. Angus Macleod[a], Cheryl E. Kennedy[b]
Blain H. Olbert[c], and J. Roger P. Angel[a,c]
[a]College of Optical Sciences, Univ. of Arizona, 1630 E. University Blvd., Tucson, AZ, USA 85721
[b]National Renewable Energy Laboratory, 1617 Cole Blvd., Golden, CO, USA 80401-3305
[c]Steward Observatory, Univ. of Arizona, 933 North Cherry Ave., Tucson, AZ, USA 85721

ABSTRACT

This paper reports methods developed to maximize the overall reflectance second-surface silvered glass. The reflectance at shorter wavelengths is increased with the aid of a dielectric enhancing layer between the silver and the glass, while at longer wavelengths it is enhanced by use of glass with negligible iron content. The calculated enhancement of reflectance, compared to unenhanced silver on standard low-iron float glass, corresponds to a 4.4% increase in reflectance averaged across the full solar spectrum, appropriate for CSP, and 2.7% for CPV systems using triple junction cells. An experimental reflector incorporating these improvements, of drawn crown glass and a silvered second-surface with dielectric boost, was measured at NREL to have 95.4% solar weighted reflectance. For comparison, non-enhanced, wet-silvered reflectors of the same 4 mm thickness show reflectance ranging from 91.6 - 94.6%, depending on iron content. A potential drawback of using iron-free drawn glass is reduced concentration in high concentration systems because of the inherent surface errors. This effect is largely mitigated for glass shaped by slumping into a concave mold, rather than by bending.

Keywords: Thin film, silver, high reflectance, concentrating, solar, mirror, reflector, CPV, CSP

1. INTRODUCTION

A number of approaches to large scale solar electricity generation require sunlight to be concentrated by reflectors. Concentrating solar systems (CSP) use flat heliostats or a cylindrical trough reflector to focus sunlight. Other systems use reflectors to concentrate sunlight onto triple-junction photovoltaic cells (CPV). To make the system cost efficient, the reflective surfaces have to be low-cost, durable and have very high reflectance to increase power output.

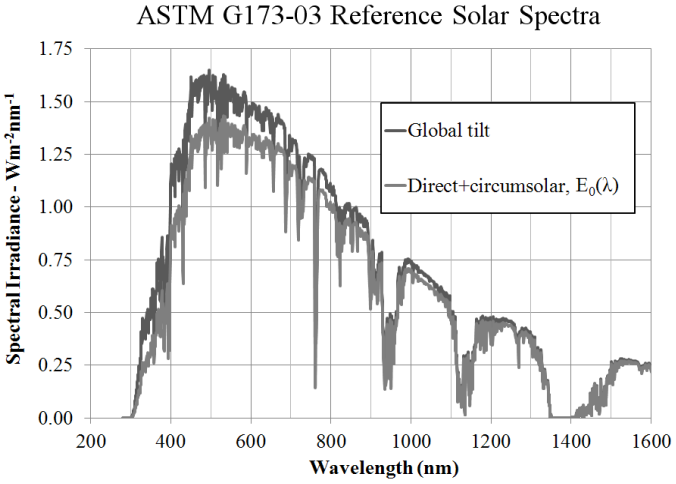

Figure 1. Global and direct + circumsolar solar spectra

Second-surface back-silvered glass reflectors are preferred for solar concentrators because of the mechanical and chemical stability of glass and the high, broad-band reflectance of silver. Glass is potentially very inexpensive when mass produced in high volume, readily available, and can be softened and shaped at high temperature. Solar reflectors made with silver deposited on the backside of glass and protected by paint are preferred by CSP and CPV solar plant suppliers

because the glass provides good protection of the silver from environmental attack. They have proven to retain their initial high reflectance for many years in the field. However, second-surface silvered glass reflectors have less than ideal reflectance for two reasons. First, the intrinsic reflectance of silver, while extremely high at visible and infrared (IR) wavelengths, drops off in the violet and ultraviolet (UV). Second, even small iron impurities in the glass cause it to absorb in the red and infrared. The 4-mm thick glass reflectors used in parabolic troughs for structural rigidity, the residual impurities in even "low-iron" float glass can absorb several percent of the reflected energy in the near infrared (NIR) wavelengths.

The efficiency of solar concentrator systems is dependent on the power conversion method. The figure of merit for CSP is the total reflected energy, i.e., reflectance averaged across the full solar spectrum weighted according to spectral intensity as shown in Figure 1. High reflectance across the full spectrum is desirable. For CPV, the current of the full triple junction cell is limited by the junction with the least current (and hence also is the output power. Typically, the shorter wavelength cells set this limit because under the typical solar spectrum, the longest wavelength junction is broader than is needed. Improved performance for CPV can thus be obtained by increasing the reflectance for the two lower cells below 900 nm.

Different materials can be used to create a highly reflective surface; metals such as aluminum (Al) or silver (Ag) are the most common candidates and have been used for centuries in optics and astronomy to make efficient mirrors. Dielectric coatings can be used, but are not as efficient over the broadband spectrum (350 to 1600 nm) that is needed to generate solar energy. The use of triple-junction cells where each junction has a specific quantum-efficiency spectrum makes CPV systems very efficient. To maximize the current, a new coating was designed using both metal and dielectric materials to increase the reflectance, given the specific spectral distribution of sunlight and to maximize the output power of the total system.

This paper will discuss the improvements that can be obtained for CPV and CSP by choosing glass with very low iron content, examine a new coating design tailored for CPV, and discuss the details of the combination of those improvements on a second-surface mirror with silver as the rear surface by comparing the theoretical performance and measurement data.

2. NOTE ON SILVER OPTICAL CONSTANTS

The primary mirror is a second-surface silvered glass, and processes to produce large silver mirrors are well known [1]. The performance of silver is critical and optimizing the coating requires an accurate knowledge of the optical constants. The optical constants of silver (n and k) are also available in the literature [2, 3]. However, depending on the method used to deposit the silver—sputtering [4], vacuum-evaporation [5], or chemical deposition [6]—the constants, and especially the real part n, can vary substantially. Evaporation is the method shown to give the lowest real index for silver, whereas chemical deposition produces the highest index and thus the lowest reflectance.

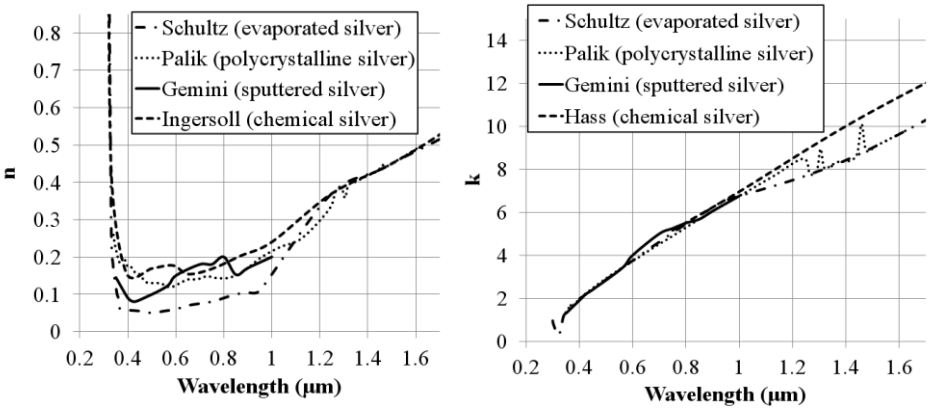

Figure 2. Optical constants of silver for various references and deposition methods

For our simulations, the constants obtained with vacuum-evaporated silver referenced in Hass [3] and measured by Schultz [7, 8] were used. We have used the constants for evaporation from Haas [3] because they are given for the widest range of wavelengths and are consistent with the values referenced in [5]. The Hass reference [3] is also more reliable

because of the distinction between the various deposition methods. The various constants found in the literature are summarized in Figure 2.

3. IRON ABSORPTION IN SECOND-SURFACE SILVERED MIRRORS

Second-surface silvered glass mirrors have been used in solar concentrating systems because of the robustness, relatively light weight, silver's high reflectance {typically, 94% average, solar-weighted hemispherical reflectance (SWV), weighted by the G173-03 solar spectrum [9]}, and reliable silver protective layer coatings. Improving the reflectance of the second-surface silvered primary mirror will allow more light to be converted into electricity.

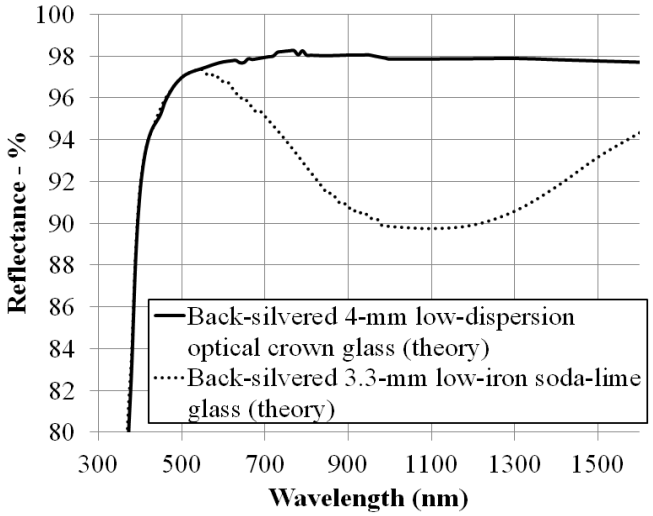

Figure 3. Theoretical reflectance enhancement gained by using optical crown glass instead of low-iron soda-lime glass

The theoretical reflectance calculated for 3.3-mm, low-iron soda-lime glass with a refractive index of 1.514 [10] and 4-mm, low-dispersion optical crown glass with a refractive index of 1.514 [11] glass is shown in Figure 3. The difference between the two glasses is their absorption coefficient which varies significantly over the solar spectrum, for example at 1 μm, $k=1.02 \times 10^{-6}$ for low-iron glass and $k=10^{-8}$ for crown glass. A very significant improvement in reflectance is obtained across the near infrared, the highest improvement being 8% at 1.1 μm wavelength. The reflectance improvement averaged over the full solar spectrum is 3.2% (see Table 1 below). This is the increase in power that would be obtained for thermal concentrator systems.

4. REFLECTOR OPTIMIZATION FOR CPV WITH TRIPLE JUNCTION CELLS

4.1 Effect of Iron Absorption on Triple Junction Cell Performance

The spectral response at 25°C of the three junctions of a typical triple junction cell is shown in Figure 4, for C1MJ cells made by Spectrolab [12]. The response of the first junction goes from 350 to 660 nm, the second from 660 to 890 nm, and the bottom subcell from 890 to 1600 nm (later generation cells have similar spectral response). Each of the three subcells also has a distinct quantum efficiency: $Q_1(\lambda)$, $Q_2(\lambda)$, and $Q_3(\lambda)$ for the top, middle, and bottom subcells, respectively.

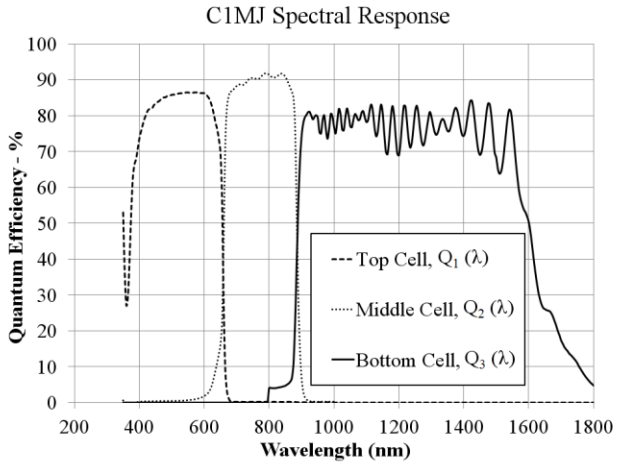

Figure 4. Triple-junction cell quantum efficiency as given by Spectrolab

Because the junctions are electrically interconnected in series in the concentrator cell, the smallest cell current limits the entire cell and is the final current flowing in the cell. As a simplified approximation, we consider direct solar radiation is reflected onto a bare cell. We take for the solar spectrum the AM 1.5 spectral irradiance $E_0(\lambda)$ of Figure 1, (obtained from SMARTS [13]). $R(\lambda)$ is the mirror reflectance and $Q_i(\lambda)$ is the quantum efficiency of the considered band i. The number of electron-hole pairs created per second in each junction is then given by integration across the optical spectrum:

$$N_i = \int_{\lambda} \frac{\lambda \cdot E_0(\lambda) \cdot R(\lambda) \cdot Q_i(\lambda)}{hc} d\lambda \qquad (1)$$

where i references the band number (1, 2 and 3).

The results for the case of no reflector (R=1) and the low iron and crown glass reflectors of Figure 3 are shown in Table 1, where the weighted flux and electron-hole pair counts are normalized to 100 total for the case with no reflector.

Table 1. Photoelectrons count before primary reflector optimization using low-iron (left) and crown (right) glass

Reflector type	**No reflector**	**Low-iron glass**	**Crown glass**
Solar weighted energy flux (black absorber)	100	93.5	97.4
Total charge carriers $N_1 + N_2 + N_3$	100	93.1	97.9
N_1	28.7	27.5	27.8
N_2	30.9	28.9	30.4
N_3	40.4	36.6	39.7

This calculation shows that in this simple approximation, with AM 1.5 solar spectrum and no reflector, the top (blue) and middle (red) junctions are reasonably balanced and provide the limit to the cell current, while the bottom junction (IR) takes a larger fraction of the spectrum than needed, with a significant excess of charge carriers. This is a well known property of this type of triple junction cell [14].

When used with a conventional reflector on low-iron glass, both the total solar-averaged reflected energy and the total number of charge carriers in all three junctions drops by 6.5% to 93.5%. However, the power output of the triple junction cell in this model is not so much reduced, as is remains limited by the current in the blue cell, which is reduced by 4.2% (down to 27.5 from 28.7). The losses from the iron absorption are confined mostly to the two longer wavelength cells, but these are not limiting the cell current. When the iron absorption is removed by switching to a crown glass substrate (column 4 of Table 1) the total, solar-averaged reflected energy is improved by 4.1%, up to 97.4% of the reference with no reflector, but the current and power from the triple junction cell, still limited by the blue junction, is improved by only 1.1% to 96.9% of the no-reflector case.

4.2 Enhancing the Reflectance for CPV with Dielectric Layers

In this section we show how the performance of second-surface silvered reflectors for CPV may be improved by addition of thin film dielectric layers between the silver and the glass back surface. Dielectric layers have been designed and used to boost the performance of front-surface silvered mirrors. For example, broad-band boosted coatings for astronomy have been previously described by Macleod in the paper by Song [15]. For our application, the layer is sandwiched between the glass and the silver, and its function is to boost reflectance in the top (blue) layer without reducing the reflectance in the other two layers to the point where they would determine the cell current. The figure of merit for the coating is to increase N_1, the photocurrent in the blue junction, without decreasing N_2 or N_3 to the point that they become less than N_1.

A simple coating we have found works well is based on a two-layer, high-low quarter wave stack, with the high index layer deposited first on the glass back surface, followed by the low index and then the silver. The thickness of the low index layer is not strictly a quarter wave, because of the silver behind it. The two common dielectric materials we have designed for are tantalum pentoxide (Ta_2O_5) for the high-index (n=2.14 at 510 nm) and silicon dioxide (SiO_2) for the low-index (n=1.45 at 510 nm). The optimum thickness for both layers is found by varying both and finding the highest value for N_1 (Equation 1). The result of this optimization is shown in the left hand diagram of Figure 6. The maximum increase in the rate of charge carrier generation in the top junction, which sets the cell current, is 1.39%, found for 52-nm thickness of Ta_2O_5, and 58-nm of SiO_2. The spectral dependence of reflectance for this boosting layer is shown in the dashed curve of Figure 5. For comparison, the unenhanced reflectance is shown as the dotted curve. The boosted layer is higher at all wavelengths between 390 and 800 nm wavelength, with a maximum boost of 1.5% at 500 nm. The changes resulting from the boosting layer in charge carrier production in all three junctions are given in the 4th column of Table 2. As can be seen, N_2 is virtually unchanged. N_3 is slightly reduced, but remains larger than N_1, and so has no effect on the cell current.

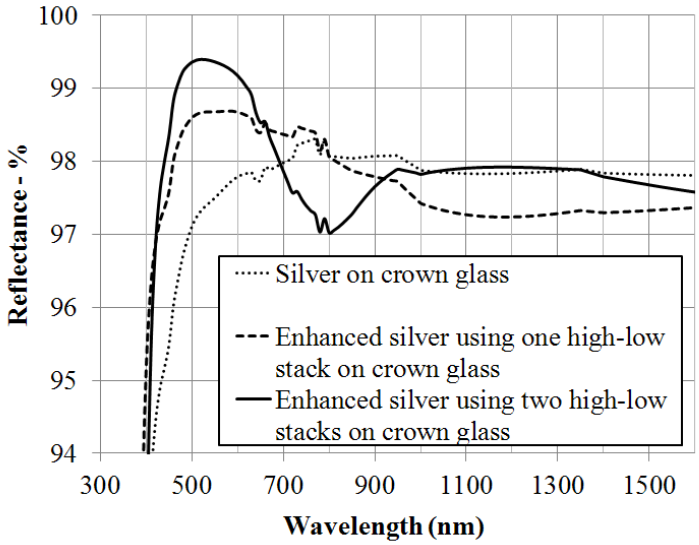

Figure 5. Reflectance of the boosted primary reflector vs. a simple second-surface silvered mirror, both using crown glass

Given this encouraging result, we have considered also the gain that could be produced with a more elaborate dielectric boost layer, a 4-layer stack with two high-low pairs. Again the thicknesses were optimized to maximize N_1. From the glass, we used 59-nm of Ta_2O5, 87-nm of SiO_2, another 59-nm of Ta_2O_5 and lastly the 58-nm of SiO_2 to match silver. The result is a small improvement, bringing the boost gain to 1.68% compared to the unenhanced silver. For the given thicknesses, the spectral reflectance in this case, depicted as the solid curve in Figure 5, shows a stronger boost over a somewhat narrower wavelength range. From Table 2 we see that N_2 in this case is slightly reduced, but not so much that the current is limited by the middle junction. N_3 is actually increased, to the same high value as for no boost. We have modeled boosting coatings with even more layers, but find little significant gain.

The combined gain for CPV of using crown instead of low iron glass (1.0 %), and the 4-layer dielectric boost (1.7%) is a gain in current and power of 2.7%.

Table 2. Photoelectrons count after performing different optimizations using crown glass

Cell type	Current triple junction				Tuned triple junction
Reflector type	**No reflector**	**Crown glass**	**Crown glass plus 2-layer coating**	**Crown glass plus 4-layer coating**	**Crown glass plus 2-layer coating**
Total charge carriers $N_1 + N_2 + N_3$	100	97.4	98.1	98.2	98.1
N_1	28.7	27.8	28.1	28.2	29.2
N_2	30.9	30.4	30.5	30.3	29.3
N_3	40.4	39.7	39.5	39.7	39.6

One more aspect of optimization we have explored is the potential for further efficiency improvement by tuning the band gap of the top cell [16] to balance N_1 and N_2 and thus increase the cell current even more. We have generated new curves for Q_1 and Q_2 like those in Figure 4 but with the crossover wavelength increased from 660 nm. We find that the values of N_1 and N_2 computed from Equation 1 for the 2-layer boosted reflectance become balanced for a crossover wavelength of 668 nm (column 6 of Table 2). N_1, and thus the cell current, is increased by 3.5%. The cell power depends also on voltage, which will be slightly reduced because of the narrower top junction band gap, but by less than 1%. Thus an increase in power output of close to 3% is indicated. In practice, cell optimization should be undertaken only when the optical transmission spectrum of the full system is known, along with on-site measurements of the solar spectrum.

4.3 Practical Design with Alumina Adhesion Layer

The adhesion of silver to glass is poor; therefore, it is common to add a layer between the silica and the silver layers to improve the adhesion. We chose a thickness of 10 nm of alumina (Al_2O_3). The thicknesses of the two boost layers were optimized as before, to maximize N_1. The result is shown in the right hand contour plot of Figure 6, and in Table 3. The maximum boost remains at 1.39%, the Ta_2O_5 layer thickness remains the same at 52 nm, but the SiO_2 layer thickness is reduced by 10 nm to 48 nm.

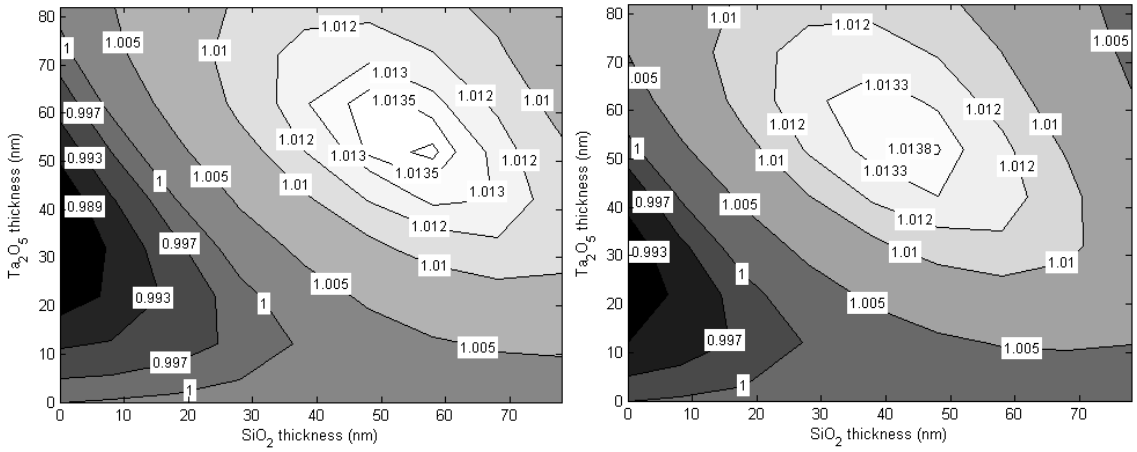

Figure 6. Optimization contour plots showing the ideal thicknesses of the two dielectrics layers for high-low index layers only (left) and with the addition of a 10-nm alumina adhesion layer (right). Contour labels are for the top layer charge carrier generation rate N1 normalized to the rate without any enhancing layers.

Table 3. Boosting layers with a single high-low stack, without and with adhesion layer

Glass	4 mm	
Ta_2O_5	52 nm	52 nm
SiO_2	58 nm	48 nm
Al_2O_3	0 nm	10 nm
Ag	100 nm	
Al_2O_3	0 nm	10 nm
Cu / Paint	200 nm	

5. EXPERIMENTAL RESULTS

5.1 Comparison with Theory

Samples of 4 mm thick low iron float and crown glass were coated commercially by electron beam evaporation, with the recipe in Table 3 that includes the 10-nm alumina adhesion layers.

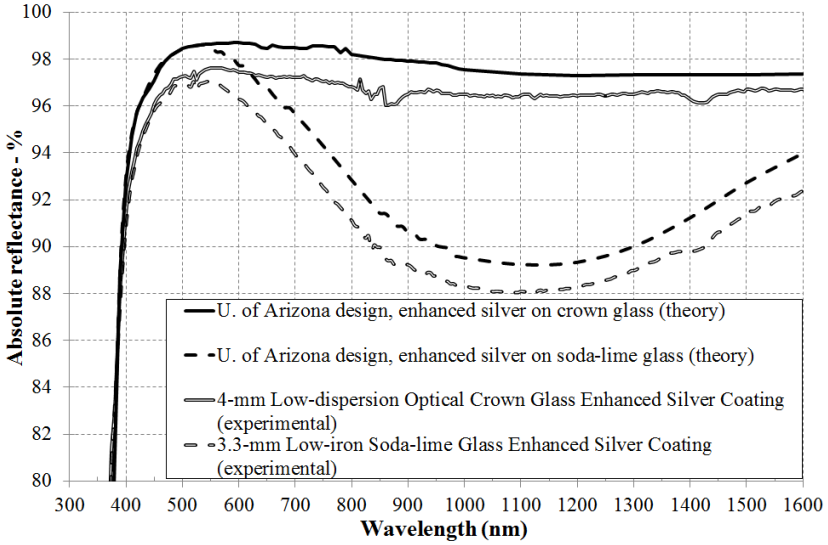

Figure 7. Spectral reflectance of University of Arizona samples, enhanced silver coating on low-iron vs. crown glass

The coated glass samples were optically characterized on a Perkin-Elmer Lambda 900 with a 60-mm integrating sphere by the National Renewable Energy Laboratory (NREL) [17]. Figure 7 shows the hemispherical reflectance for the two glass samples—both as measured and the theoretical curves of the design. The 2σ (95.4% confidence level) uncertainty in the measured reflectance (R) at a specific wavelength (λ) is ± 0.4% of the measured value over the spectral range of interest, λ= 300 to 500 nm, or the measured reflectance ± (Rx0.4)% for each λ. The largest contribution to the 2σ standard deviation occurs at the sharp transition in the silver spectrum where the reflectance of silver rapidly drops between 380 and 320 nm. This value approximates the standard deviation (σ) at the sharp transition or when R(λ) is small, but is closer than assigning a strict value (e.g. = 0.4%).

The highest measured reflectance for the boosted sample on crown glass is 97.5±0.4% at 550 nm, and the reflectance stays above 96% between 420 nm and 1600 nm. The solar weighted reflectance is 95.4%. The low iron glass sample has much reduced reflectivity in the near infrared. The difference in reflectivity between the two glasses follows theory with a predicted absorption coefficient of about 10% at 1 μm for the low-iron glass. However, the measurements for both the crown and low-iron samples fall about 1% below the theoretical value in the visible, 2% around 1 μm, and 1% in the IR. We have considered a number of possible causes for this offset.

1) Absorption in the crown glass from residual iron or other impurities could be responsible in part.
2) Errors in the optical constants of the materials used can affect the final reflectance. The accuracy of the constants for glass and dielectric materials was checked using the available literature on optical constants for evaporated materials, and only silver can be argued to vary in a significant way. As described in subsection 2.5, silver

constants vary according to the deposition method; with the refractive index n has a greater variation compared to k (Figure 3). The experimental data depict a better fit to the design if we use the data from Palik [2] for the silver constants. However, the silver from Palik [2] is polycrystalline, which is not the expected form for the coating used.

3) Thickness errors in the dielectric layers are not likely to cause the discrepancy. They were deposited with 5% accuracy. We have found by modifying the layer thicknesses in the optical model that the reflectance can vary by 2% between 350 and 400 nm, by about 1% between 400 and 430 nm, and does not vary by more than 0.5% after 430 nm. As a result, the deposition method should not cause the variation that we observe in the above Figure.

4) The measurement method can also cause some errors. Measuring reflectance with accuracy is not a simple task. The best reflectance measurement accuracy published is 0.1% by Bennett [18]. Calibrating an instrument to measure in the 5% range is relatively easy, but it is difficult in the 1% range and very difficult in the 0.1% range.

5.2 Comparison with Other Second-Surface Silvered Samples

In Figure 8 the spectral reflectance measurements for the University of Arizona crown glass reflectance sample are compared to measurements made also at NREL of other second-surface silvered glass reflectors used for solar application, all low-iron, but with some variation in them. Our design deposited on the crown glass shows the highest reflectance of all the samples from 400 to 1600 nm by > 1%, The measured solar weighted reflectance of our coating, 95.4%, is greater than non-enhanced, wet-silvered, 4-mm low-iron glass mirrors whose reflectance ranges from 91.6 - 94.6%, depending on the purity of the low-iron glass. The reflectance of the glass coated with the UA design is also higher for wavelength from 400 to 600 nm, which corresponds to an increase in the top, current limiting CPV cell band.

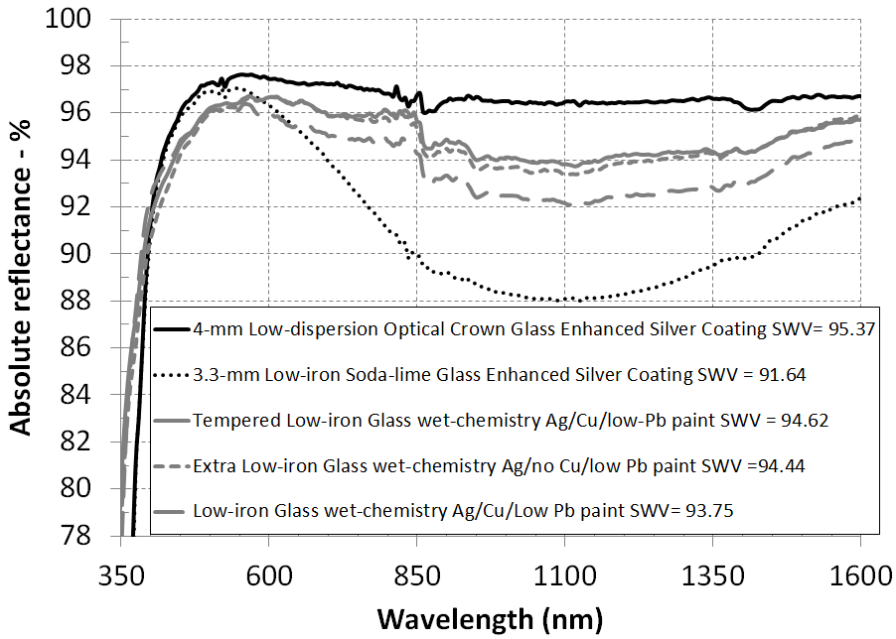

Figure 8. Performance of University of Arizona enhanced silver coating compared to existing second-surface silvered, low-iron glass

6. DISCUSSION AND CONCLUSION

In this paper, we have explored two ways to increase the reflectance of second-surface silvered glass reflectors for solar concentrating optics. The first way is to eliminate the residual absorption of the glass, by using drawn crown glass instead of low-iron float, which has significant iron content. The second way is to deposit a boosting layer between the second glass surface and the silver. A design to enhance the blue and violet part of the spectrum has been developed, aimed at improving the power of CPV systems using triple junction cells, whose output is limited by the solar flux at shorter wavelengths. Samples of reflectors thus enhanced were measured at NREL. The measured reflectance reaches as high as

97.5% at 500 nm. The solar-weighted reflectance for CSP applications is 95.4%, higher than a reflectance measured for wet-silvered samples on various low-iron float glasses.

A potential drawback for optical crown glass with negligible iron absorption is its current availability only as drawn glass, a form not generally used for solar reflectors, in part because the drawing process results in less uniform thickness than the low-iron float process. This difficulty is overcome in the method of manufacture developed at the University of Arizona, in which the glass is shaped not by bending but by molding, so that the backside surface to be silvered is formed against a mold of the correct shape, independent of thickness variations. Thickness variations remain, but they are transferred to the front, refracting surface of the glass, where their effect on optical quality of the reflector is diminished.

7. ACKNOWLEDGEMENTS

We gratefully acknowledge support from the DOE under award DE-FG36-08-GO88002, from Science Foundation Arizona, the Cottrell Foundation, and from REhnu LLC. This work was supported by the U.S. Department of Energy under Contract No. DE-AC36-08-GO28308 with the National Renewable Energy Laboratory.

REFERENCES

[1] R. Wilson, *Reflecting telescope optics II*, chapter 6, 423-448, Springer-Verlag, Berlin, 1999.
[2] E. D. Palik, *Handbook of Optical Constants of Solids*, Academic Press Inc. (1985).
[3] G. Hass and L. Hadley, "Optical Constants of Metals", in *American Institute of Physics Handbook*, D. E. Gray, Ed. (McGraw-Hill, New York, 1972), pp. 6-124–6-156.
[4] Maxime Boccas, Tomislav Vucina, Claudio Araya, Esteban Vera, Clayton Ahlee, "Coating the 8-m Gemini telescopes with protected silver", Proc. SPIE 5494, 239 (2004).
[5] R. H. Huebner, E. T. Arakawa, R. A. MacRae, and R. N. Hamm, "Optical Constants of Vacuum-Evaporated Silver Films", *Journal of the Optical Society of America*, Vol. 54, No. 12, pp. 1434-1437 (1964).
[6] L. R. Ingersoll, *Astronomical Physics*, pp. 284-285.
[7] L. G. Schultz, "The Optical Constants of Silver, Gold, Copper, and Aluminum. I. The Absorption Coefficient k", *Journal of the Optical Society of America*, Vol. 44, No. 5, pp. 357-362 (1954).
[8] L. G. Schultz, "Optical Constants of Silver, Gold, Copper, and Aluminum. II. The Index of Refraction n", *Journal of the Optical Society of America*, Vol. 44, No. 5, pp. 362-368 (1954).
[9] ASTM G173-03, *Terrestrial Reference Spectra for Photovoltaic Performance Evaluation*, American Society for Testing and Materials, 2003.
[10] M. Rubin, "Optical Properties of Soda-Lime Silica Glasses", in *Solar Energy Materials*, Vol. 12, pp. 275-288 (1985).
[11] http://www.reichmann-feinoptik.com/assets/applets/B_270®_Superwite_e.pdf
[12] Spectrolab, private communication.
[13] http://www.nrel.gov/rredc/smarts/
[14] Geoffrey S. Kinsey and Kenneth M. Edmondson, "Spectral Response and Energy Output of Concentrator Multijunction Solar Cells", *Progress in Photovoltaics: Research and Applications* 2009; 17:279-288.
[15] Dar-Yuan Song, R. W. Sprague, H. Angus Macleod, and Michael R. Jacobson, "Progress in the development of a durable silver-based high-reflectance coating for astronomical telescopes", *Applied Optics*, Vol. 24, No. 8, pp. 1164-1170 (1985).
[16] A. Dobbin, M. Lumb, and T. N. D. Tibbits, "Modeling of location specific solar spectra for use in the tuning of multi-junction solar cells and energy harvest predictions", *Proc. 5th World Conf. Photovolt. Energy Conversion*, 2010.
[17] http://www.nrel.gov/
[18] Jean M. Bennett and E. J. Ashley, "Calibration of Instruments Measuring Reflectance and Transmittance", *Applied Optics*, Vol. 11, No. 8, pp. 1749-1755 (1972).